

Article

Wound Healing Activity of the Flavonoid-Enriched Fraction of *Selaginella bryopteris* Linn. against Streptozocin-Induced Diabetes in Rats

Arti Gautam ¹, Vikas Kumar ¹, Lubna Azmi ², Ch. V. Rao ³, Mohammed Moizuddin Khan ⁴ , Beenish Mukhtar ^{4,5}, Mehnaz Kamal ⁶ , Muhammad Arif ⁷, Seema Mehdi ⁸, Saud M. Alsanad ⁹ , Osama A. Al-Khamees ⁹ , Talha Jawaid ^{9,*} and Aftab Alam ¹⁰ 

- ¹ Department of Pharmaceutical Sciences, Sam Higginbottom University of Agriculture, Technology and Sciences (SHUATS), Prayagraj 211007, Uttar Pradesh, India
 - ² Department of Pharmaceutical Chemistry, Institute of Pharmaceutical Science, University of Lucknow, Lucknow 226007, Uttar Pradesh, India
 - ³ Pharmacology Division, National Botanical Research Institute (CSIR), Lucknow 226001, Uttar Pradesh, India
 - ⁴ Department of Basic Medical Sciences, College of Medicine, Dar Al Uloom University, Riyadh 13314, Saudi Arabia
 - ⁵ Department of Physiology, Santosh Deemed to be University, Ghaziabad 201009, Uttar Pradesh, India
 - ⁶ Department of Pharmaceutical Chemistry, College of Pharmacy, Prince Sattam bin Abdulaziz University, Al-Kharj 11942, Saudi Arabia
 - ⁷ Faculty of Pharmacy, Integral University, Kursi Road, Lucknow 226026, Uttar Pradesh, India
 - ⁸ Department of Pharmacology, JSS College of Pharmacy, JSS Academy of Higher Education and Research, Mysuru 570004, Karnataka, India
 - ⁹ Department of Pharmacology, College of Medicine, Imam Mohammad ibn Saud Islamic University (IMSIU), Riyadh 13317, Saudi Arabia
 - ¹⁰ Department of Pharmacognosy, College of Pharmacy, Prince Sattam bin Abdulaziz University, Al-Kharj 11942, Saudi Arabia
- * Correspondence: tjkhan@imamu.edu.sa



Citation: Gautam, A.; Kumar, V.; Azmi, L.; Rao, C.V.; Khan, M.M.; Mukhtar, B.; Kamal, M.; Arif, M.; Mehdi, S.; Alsanad, S.M.; et al. Wound Healing Activity of the Flavonoid-Enriched Fraction of *Selaginella bryopteris* Linn. against Streptozocin-Induced Diabetes in Rats. *Separations* **2023**, *10*, 166. <https://doi.org/10.3390/separations10030166>

Academic Editors: Frank L. Dorman, Isaac Rodríguez, Danilo Sciarrone and Victoria Samanidou

Received: 31 December 2022
Revised: 15 February 2023
Accepted: 21 February 2023
Published: 28 February 2023



Copyright: © 2023 by the authors. Licensee MDPI, Basel, Switzerland. This article is an open access article distributed under the terms and conditions of the Creative Commons Attribution (CC BY) license (<https://creativecommons.org/licenses/by/4.0/>).

Abstract: Diabetes and its complications, such as delayed wound healing, are increasing at an alarming rate in India, putting an enormous strain on the country's limited healthcare resources. Hence, the present study proposes to screen/identify the possible mechanisms and to study the effect of the flavonoid-enriched fraction of *Selaginella bryopteris* extract against human keratinocyte cell lines (HaCaT) and streptozocin (STZ)-induced diabetic wounds in a male Wistar rat model. Chemical profiling was performed by an MTT assay. The obtained GC–MS analysis results showed the presence of amentoflavone, gallic acid, imidazole, palmitic acid, catechine, L-fucitol, lupeol, and myo-inositol as the major bioactive phytoconstituents. *S. bryopteris* induces the generation of ROS, the condensation of chromatin in the nucleus, and changes in the membrane potential of mitochondria in HaCaT cell lines. An *S. bryopteris*-dependent induction of apoptosis-mediated cell death in HaCaT cell lines was confirmed by an AO/PI analysis. Mitochondrial depolarization was reflected in JC-1 staining of cells. The wound size was reduced and epithelialization was enhanced. Keratinocyte migration decreased interleukins, TNF- α , IL-2, and IL-6 and the expression of pro-apoptotic (p53, caspase-3, caspase-9, and Bax) and anti-apoptotic (Bcl-2) genes in a dose-dependent manner. Keratinocyte migration increased antioxidant enzyme levels (CAT, SOD, MDA, and GSH). Wound healing is facilitated through the mitochondria-mediated apoptosis pathway, revealing a new area of diabetic wound therapy.

Keywords: *Selaginella bryopteris*; streptozocin; antioxidants; interleukins

1. Introduction

India, after China, has the second highest percentage of diabetic patients worldwide. There were over 72 million cases of diabetes in 2017 in India and the number is projected to rise to 125 million by 2040 [1]. A total of 175 million people with diabetes are undiagnosed

and 15% of people have chronic wounds related to diabetes. Wounds impact 7–9% of the population globally, drastically lowering their quality of life. The profits of advanced wound care products are expected to reach around USD 9.4 billion by 2022. Delayed wound healing in diabetic patients arises through several factors, such as poor vascular supply in the hemostasis phase, slow recruitment of neutrophils in the inflammation phase, reduced tensile strength, reduced collagen deposition, and reduced fibroblast activity in the proliferation phase. As we know, several pharmacological models have been reported to understand the mechanism of poor wound healing. Streptozocin is a naturally occurring alkylating antineoplastic agent used in medical research and in high doses is responsible for inducing hyperglycemia in animal models, which leads to elevated blood sugar levels, aggravates the diabetic condition, and extends the expression of TNF- α , all leading to impaired wound healing. A wound analysis in diabetic rats has shown that the level of TNF- α is three times higher compared to normal rats. Cellular apoptosis and the least expression of the wound healing process is deregulated by the Bcl-2 protein [2]. Reactive oxygen species increase the expression of proapoptotic proteins such as BAX, FAS, and caspases, while decreasing the expression of anti-apoptotic proteins such as B cell lymphoma 2 genes (Bcl-2) [3]. Diabetic wound complications are even more poorly addressed. There is an urgent need to develop alternatives to treat diabetic wounds which are aimed at specific targets or a follow a mechanism-based wound healing approach. As we know, several pharmacological models have been reported to understand the mechanism of poor wound healing in diabetic models of Wistar rats with excision and incision wounds. By using the antibiotic streptozocin, a naturally occurring alkylating antineoplastic agent used in medical research, hyperglycemia was induced in animal models, which led to elevated blood sugar levels.

On the basis of the previous literature, several ethnobotanical plants, viz. *Rosmarinus officinalis*, *Sparassis crispa*, *Carica papaya*, and *Cymbopogon nardus*, are reported as wound healing agents against diabetic wounds [4–7]. *S. bryopteris* a a traditional magical herb used for several health care isshue like diabetes inflammation but there no scientific data reported regarding its activity on wound healing ”.

S. bryopteris, also known as Mrit Sanjeevani, is mentioned in The *Ramayana* for its magical medicinal properties. This herb (often known as Sanjeevani) is widely used as a natural cure for a variety of ailments in tribal India [7,8]. *S. bryopteris* is rich in flavonoid compounds. We draw particular attention to amentoflavone and 8-aryl flavonoid because of their valuable, potent antioxidant activities. *S. bryopteris*’ reported biological activities include anti-bacterial, anti-protozoal [8–10], anti-plasmodial, leishmanicidal, and anti-depressant properties, and it is also used for heat stroke [11–13]. Some previous studies have also revealed its role against skin inflammatory diseases [14]. Traditionally, *S. bryopteris* has been used as an aqueous leachate for treating a number of health complications such as hot flushes, a burning sensation during micturition, jaundice, etc. It is also given orally to pregnant women for relieving pain during delivery [9,15]. The current strategy incorporates the approaches of conventional systems of medicine, such as Ayurveda, with the present knowledge of medicines, tools, and techniques to verify the claimed therapeutic benefits of *S. bryopteris*. We also quantify the effects of *S. bryopteris* in stimulating several factors which are responsible in wound healing using in vitro and in vivo models.

2. Material and Methods

2.1. Reagents

MTT (3-(4,5-dimethylthiazol-2-yl)- 2,5-diphenyltetrazolium bromide) and all the dyes (acridine orange (AO), propium iodide (PI), JC-1, and (DAPI) 4’, 6-diamino-2-phenylindole) were procured from Himedia Pvt. Ltd. (Mumbai, India). STZ (Streptozocin) was purchased from Sigma Aldrich (St. Louis, MO, USA). Biochemical reagent kits and the ELISA kit were procured from Transasia Bio-Medicals Ltd. (Mumbai, India) and Elabscience (Wuhan, China). Analytical grade chemicals and reagents were used for all the analyses, and were procured from Merck and Himedia Lab Pvt. Ltd. (Mumbai, India).

2.2. Extract Preparation and Phytochemical Profiling

K. Madhava Chetty, of Venkateshwara University, Tirupati, India, certified the plant material, constituting the entire plant (specimen no. 1098), obtained from Chitrakoot, Madhya Pradesh. The samples were shade-dried and extracted with ethanol/petroleum ether (70:30% *v/v*) for 48 h. The extract was concentrated using a rotary evaporator before being lyophilized. The lyophilized crude extract was separated with different polarity solvents (hexane, chloroform, and ethyl acetate). The most bioactive ethyl acetate fraction SBE was selected based on its high antioxidant activity, with an IC₅₀ of 17.4 µg/mL, compared to IC₅₀ of standard flavonoid which was initially analyzed. The methods given by Ragazzi and Veronese and Oyaizu were used to estimate the total phenol content (TPC) and total flavonoid content (TFC), respectively [11,16]. The TPC and TFC were expressed as gallic acid equivalent (GAE)/gram and as mg quercetin equivalent (QE)/gram [16,17], correspondingly. A GC-MS analysis was used to characterize the phytochemical properties of the bioactive fraction of *S. bryopteris* utilizing N-methyl-N-(trimethylsilyl) trifluoroacetamide (MSTFA) as the derivatizing agent. The derivatized material was investigated using GC-MS (Thermo Trace GC Ultra) and a mass spectrometer (Thermo Fisher, Waltham, MA, USA, DSQ II). The data were recorded using a mass selective detector. The detector was set to operate in electron impact mode (ionization energy: 70 eV, ionization current: 2.0 mA, mass range: 50–800 *m/z*). The resulting chromatographic and mass data were collected using the Xcalibur program. The *m/z* ratio for each metabolite fragment was investigated using GC-MS spectral library databases such as WILLY and NIST. For the discovered metabolites, the relative concentration was represented as a percentage of peak area [18].

2.3. In Vitro Wound Healing Studies

2.3.1. Cell Culture

Aakaar Biotechnologies Pvt Ltd., Lucknow, provided the cell line, with a passage number of 8, used in this investigation. RPMI 1640 medium, 10% fetal bovine serum (heat-inactivated), and antibiotic solution (100 U/mL penicillin and 100 g/mL streptomycin) were used to culture HaCaT cells. The cells were grown at 37 °C in a humidified environment containing 5% carbon dioxide. Once the cells had grown significantly, they were trypsinized in trypsin-EDTA and counted using a hemocytometer.

2.3.2. MTT Assay

An MTT assay was used to determine the effect of *S. bryopteris* on cell growth [19]. For 24 h, different quantities of *S. bryopteris*, ranging from 0 to 80 µg/mL, were tested in 96-well sterile plates. Control cells and cells treated with the standard were placed in opposition (betadine). After 24 h, the medium was replaced in each well with 20 µL sample and MTT was done after 2 h. The liquid for dissolving formazan crystals was then dissolved in 1% DMSO. This was followed by a 30 min incubation period with an IC₅₀ value of 17.5 µg/mL. The absorbance at 570 nm was measured using a microplate reader (Model 680 XR Bio-Rad laboratories Inc.).

2.3.3. Assessment of Nitric Oxide (NO)

For assessing the impact of *S. bryopteris* on oxidative stress, HaCaT cells were cultured in different concentrations ranging from 0 to 60 µg/mL for a duration of 24 h. The cells were then stained with dichlorofluorescein diacetate (DCFH-DA), with the final concentration held at 20 M for 15 min. This will determine the status of the intracellular reactive oxygen species. Phosphate-buffered saline was used to wash the cells three times for examination under a fluorescent microscope. Griess reagent was employed to measure the nitrite content to determine the nitric oxide production. Briefly, the absorbance was checked after mixing the Griess reagent (50 µL) in 50 µL of culture medium containing cell culture (with or without *S. bryopteris*) and incubating it for 20 min. The absorbance was observed at 520nm.

2.3.4. Assessment of Cell Organelles Health Parameters Nuclear Morphology Analysis Using DAPI Staining

This staining technique was employed to record the changes in nuclear morphology. For this analysis, cells were incubated overnight in a cover slip placed in six-well plates. After that, cells (3×10^5) were treated with varying concentrations (0–60 $\mu\text{g}/\text{mL}$) for 24 h. At the final concentration (2 $\mu\text{g}/\text{mL}$), cells were stained with DAPI for 15 min (Elabscience, software and performed at CSIR Lab, lucknow, India). Staining was followed by three washes with phosphate-buffered saline to remove excess dye. Under a fluorescence microscope, UV filters were used to observe the marked cells.

Mitochondrial Membrane Potential Analysis Using JC-1 Staining

The principle behind JC-1 staining is that JC-1 dye aggregation is reduced by mitochondrial depolarization. This, in turn, causes augmented green fluorescence due to the presence of JC-1 monomers. Cells were cultured overnight in a multi-well plate with different concentrations of *S. bryopteris* (0–60 g/mL) for this study. JC-1 staining solution (5 g/mL) was applied to each well and incubated for 30 min at 37 °C in a carbon dioxide incubator. After that, the samples were cleaned with assay buffer and fixed in the BD cytofix/cytoperm assay kit. This plate was then incubated in the dark for 15 min. Cells were rinsed with phosphate-buffered saline three more times, and pictures were captured using an inverted fluorescence microscope (Nikon LeicaM165 FC) [19].

Morphological Evaluation for Apoptosis

Acridine orange/propidium iodide (AO/PI) stain was employed to record the effects of *S. bryopteris* on apoptosis [20]. For this analysis, cells were incubated overnight in a cover slip placed in six-well plates. Cells (3×10^5) were then treated with different concentrations (0–60 g/mL) and kept for 24 h under physiological conditions. Cells were stained for 15 min with a freshly produced combination of AO/PI at a final concentration of 10 g/mL. Staining was followed by three washes with phosphate-buffered saline to remove excess dye. Under a fluorescence microscope, UV filters were used to observe the marked cells.

2.4. In Vivo Wound Healing Study

2.4.1. Experimental Animals and Protocol

A total of 32 male Wistar rats were used weighing around 100–120 g. Animals were arbitrarily separated into four groups, each group containing eight animals for incision wound models.

Group I: Kept as normal control and were given 0.9% normal saline (1 mL/kg, p.o.);

Group II: Kept as toxic control and were given STZ (60 mg/kg, p.o.);

Groups III and IV: Kept as drug-treated groups and were given *S. bryopteris* (0.5% w/w topically + STZ 60 mg/kg, i.p.) and *S. bryopteris* (0.10% w/w topically + STZ 60 mg/kg, i.p.), respectively.

Group V: Kept as the standard group and were given betadine (0.5% w/w topically + STZ 60 mg/kg). Animals were kept in an animal house and ideal conditions of feed and water were maintained. The Institutional Animal Ethics Committee gave its approval to all methods used for animal experiments, and they all followed the CPCSEA (1732/GO/Re/s/13/CPCSEA), which was established by the CSIR-NBRI in Lucknow. Animals were given a Zoletil–Rompun mixture as an anesthetic during the procedure to remove the skin from lesions at the end of the trial. The skin collected was stored at 80 °C for later analysis.

2.4.2. Effect of Selaginella bryopteris on Antioxidant Parameters

Tissue collected from lesions was homogenized and centrifuged for 15 min at 10,000 rpm and 4 °C temperature. The obtained supernatant was used to evaluate different antioxidant markers such as catalase (CAT), malonaldehyde (MDA), glutathione (GSH), and superoxide dismutase (SOD).

2.4.3. Assessment of Cytokine Levels in Wounded Tissue

Interleukins IL-6, IL-2, and TNF- α were examined using the protocols given by the assay kits (Elabscience Biotech Co. Ltd. Wuhan, Hubei, China). IL-2, IL-6, and TNF- α were evaluated using the assay kit's methods (Elabscience Biotech Co. Ltd. Wuhan, Hubei, China).

2.5. Histological Analysis

Tissue obtained from lesions was embedded into paraffin wax. For histological examination, thin sections of 4 mm thickness were cut. These thin sections were then deparaffinized using xylene. A gradient of alcohol solution was employed to rehydrate the deparaffinized tissue, which was then stained with hematoxylin and eosin (H&E) dye. An Olympus microscope (magnification, 200; Olympus India, Mumbai, India) was used to visualize the stained slides.

2.6. Gene Expression Study via Quantitative Real-Time PCR

RNA was isolated using the TRIzol reagent. The isolated RNA's quality and concentration were predicted using the Nano-drop device at 260/280 nm. The total extracted RNA was used to create cDNA using the Enhanced Avian HS RT-PCR kit from Sigma Aldrich in the United States. The generated cDNA served as a template for qRT-PCR to roughly represent the entire transcript level. SYBR Green PCR Master Mix (Applied Biosystems, Waltham, MA, USA) was used in a StepOne Real-Time PCR system (Applied Biosystems, USA). To assess the quantitative real-time expression of genes, the 2-ct approach was used. Ellman was cited in the invention of the primer sequence for each individual gene [21].

2.7. Statistical Analysis

The results of the experiments are depicted as the mean of five replicates. Using Duncan's multiple range test (DMRT), the significant variance between means ($p < 0.05$) was determined. The standard deviation was calculated as the average of the five replicates.

3. Results and Discussion

3.1. Phytochemical Profiling *Selaginella bryopteris*

The yield of flavonoid and flavonoid contents for the 70% ethanolic extract of *S. bryopteris* was 17.71% *w/w*. The total flavonoid content was 150 ± 6.19 (mg QE eq./gram *S. bryopteris*). A GC-MS analysis was carried out on the ethyl acetate fraction of *S. bryopteris*. Seven main pharmacologically active compounds were identified from the flavonoid fraction of the plant extract. These important substances included catechine, L-fucitol, lupeol, amentoflavone, gallic acid, imidazole, palmitic acid, and myo-inositol. Figure 1 shows the peak areas for the following compounds: imidazole (37.8 4.20), gallic acid (7.3 0.87), catechine (0.41 0.12), amentoflavone (8.87 1.55), palmitic acid (1.3 0.65), L-fucitol (5.9 1.40), lupeol (1.1 0.68), and myo-inositol (6.7 *S. bryopteris* extract is a specialized natural remedy for treating diabetic wounds). In the GC-MS study of *S. bryopteris*, several pharmacologically active substances, including palmitic acid, imidazole, gallic acid, lupeol, amentoflavone, L-fucitol, myo-inositol, and scyllo-inositol, have been identified. Anticancer properties have been reported for imidazole (an alkaloid) and amentoflavone (flavonoid); wound healing properties have been found in lupeol (triterpenoid), gallic acid (flavonoid compound), and palmitic acid (naturally occurring fatty acid); and gallic acid also possess antioxidant properties [14].

3.2. In Vitro Wound Healing Study

When used against HaCaT cell lines, *S. bryopteris* demonstrates wound healing activities. In this instance, an MTT test has been utilized to evaluate cell viability. *S. bryopteris* transformed MTT into formazan crystals, which are insoluble (purple colored). The results of the assay showed that the cell viability drastically reduced with a rising concentration of *S. bryopteris* in the range of 10–80 $\mu\text{g/mL}$. The IC_{50} for *S. bryopteris* was found to be 17.29 μM

from the MTT assay, Figure 2A. The MTT assay was used to examine the anti-proliferative activity of *S. bryopteris* initially and the results were justified using AO/PI staining by employing a flow-cytometric analysis in a dose-dependent manner. In the PI region, PI staining shows that 45.02% of HaCaT cells are present. In comparison, only 6.14% of control cells exhibit a strong anti-proliferative effect from *S. bryopteris*.

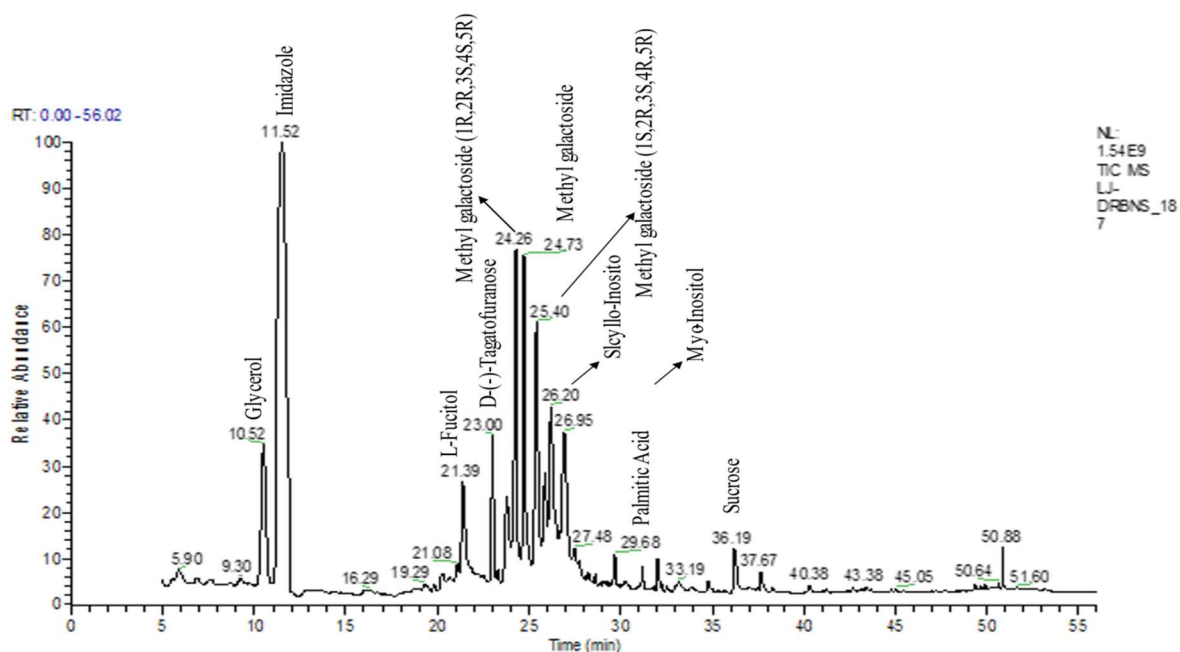


Figure 1. GC-MS chromatogram represents the bioactive compounds identified in the flavonoid enriched fraction of *S. bryopteris*.

3.2.1. Selaginella bryopteris Induces Oxidative Stress in HaCaT Cells

Excessive production of nitric oxide in the cells causes cell mortality. *S. bryopteris* amplified NO generation in a concentration-dependent pattern. At different concentrations of *S. bryopteris*, i.e., at 60, 40, and 20 $\mu\text{g}/\text{mL}$, NO production was 122%, 82%, and 42%, respectively, Figure 2B. In the ROS analysis, the fold change of the fluorescence intensity of cells was gradually increased when the concentration of PLE was increased, Figure 2C. JC-1 staining was used to examine mitochondrial dysregulation. JC-1 fluoresces red in the case of normal mitochondria and green in the case of damaged mitochondria (depolarized). A flow cytometric investigation reflected a shift in cell density towards the green channel after *S. bryopteris* treatment, Figure 2D. Through AO/PI staining and fluorescence microscopy, the morphological alterations brought on by apoptosis were evaluated. The lipophilic cationic dye JC-1 was employed to measure the potential of the mitochondrial membrane. A loss in membrane potential, a hallmark of apoptosis, prevents JC-1 from accumulating as red fluorescent J-aggregates in the mitochondria of the extremely penetrable apoptotic cells.

3.2.2. Selaginella bryopteris Causes Apoptotic-Mediated Cell Death

Indicators of apoptosis-induced cell death also include altered mitochondrial function and disturbed chromatin condensation. AO/PI staining gave a preliminary confirmation of the initiation of apoptosis. The nucleic acid of both dead and alive takes up acridine orange, while propidium iodide is taken up only by cells with depleted membrane integrity. Apoptotic cells are dyed fully green, making it easy to distinguish between them and living cells, while the presence of propidium iodide causes apoptotic cells to appear yellow to orange, depending on the degree of membrane integrity depletion. The *S. bryopteris* content increased with the appearance of yellow-orange-stained apoptotic cells (Figure 3A).

3.2.3. Selaginella bryopteris Affects Cell Organelle Health in HaCaT Cells

The impacts of reactive oxygen species on cellular organelles include dysregulation of mitochondria, defects in the condensation of chromatin, and modification of nucleus fragmentation. Aberrations in chromatin condensation were detected by DAPI staining. Chromatin condensation is reflected by augmented fluorescence intensity. At 20, 40, and 60 $\mu\text{g}/\text{mL}$ concentrations of *S. bryopteris*, the fluorescence intensity gradually increased, Figure 3b. Microscopic images from DAPI staining depicted a strong relation with flow cytometric analysis, confirming the fact that *S. bryopteris* causes mitochondrial dysregulation. Figure 3c, shows that *S. bryopteris* caused mitochondrial depolarization in a concentration-dependent manner. Eventually, cell DAPI labeling and flow cytometry were used to investigate the cell cycle phase distribution.

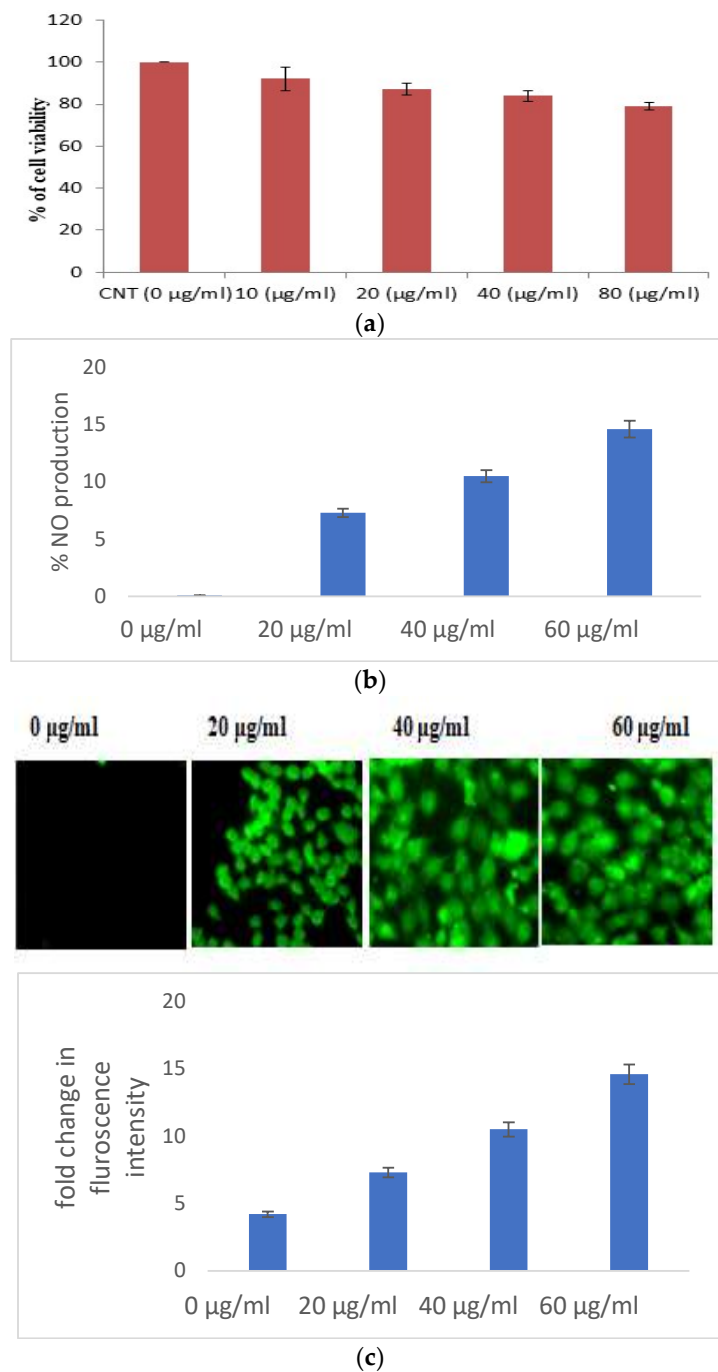


Figure 2. Cont.

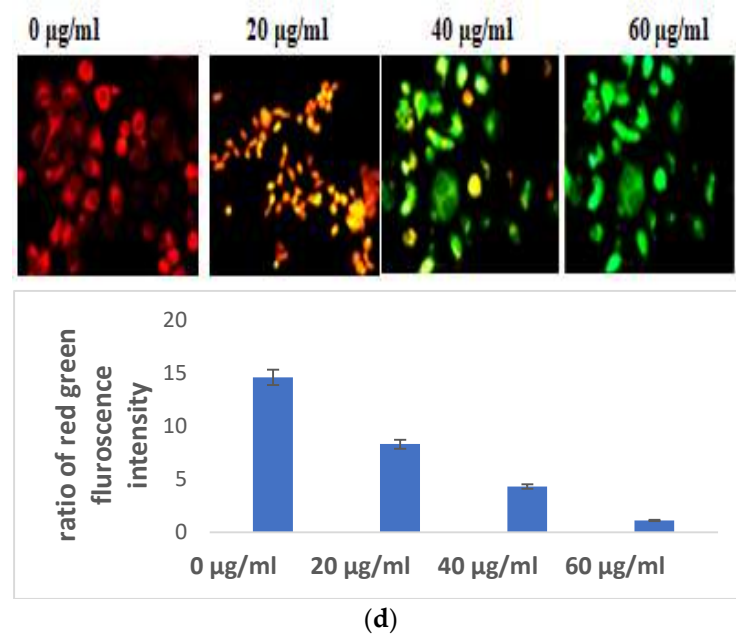


Figure 2. (a) Cell viability of HaCaT cells in the presence/absence of *S. bryopteris*, as determined by an MTT assay. (b) Analysis of the release of nitric oxide in the culture supernatant, as estimated by Griess reagent. (c) Analysis of the generation of reactive oxygen species in HaCaT cells in the presence/absence of *S. bryopteris*, as determined by DCF-DA staining. (d) Analysis of the mitochondrial health of HaCaT cells in the presence/absence of *S. bryopteris* after JC-1 staining.

3.3. In Vivo Study

3.3.1. Antioxidant Markers

Oxidative stress is directly proportional to the generation of reactive oxygen species. Oxidative damage is the chief factor for the pathogenesis of several “ailments”. The photograph of animals was shown in Figure 4a, and the analysis of wound area were given in Figure 4b. The levels of TBAR (thiobarbituric acid reactive substances) (0.26 ± 0.02 nM of MDA/ μ g of protein) was decreased by *S. bryopteris* (Figure 5A). The GSH levels were improved (1.10 ± 0.06 mg%) and then non-significantly reduced following STZ treatment (1.04 ± 0.07 mg%), in the case of the control. In contrast, GSH levels were augmented (1.4 ± 0.04 mg%) after treatment with *S. bryopteris* (Figure 5B). The STZ-treated group showed a reduction in the levels of SOD (0.023 ± 0.002 units of SOD/mg of protein) and CAT (14.40 ± 0.97 nM of H_2O_2 /min/mg of protein), which were regained after treatment with *S. BRYOPTERIS* (i.e., 0.031 ± 0.007 units of SOD/mg of protein and 40.59 ± 0.75 nM of H_2O_2 /mg of protein), Figure 5C-D. Additionally, in an STZ-induced diabetic rat model system, we assessed the effect of topical administration of *S. bryopteris* on promoting wound healing and compared it to betadine, a positive control. Betadine has been touted as a promising drug for the avoidance of side effects in treating and preventing diabetic wounds. The development of chronic problems of diabetes mellitus caused by STZ is mostly attributed to the elevated level of oxidative stress that is linked with the disease. Cells are shielded from oxidative damage by antioxidants such as reduced glutathione (GSH), superoxide dismutase (SOD), and catalase. In our own publication, we demonstrated that type 2 diabetes mellitus patients experience increased levels of oxidative stress.

3.3.2. Elisa Quantified Interleukins and TNF- α

In the pathogenesis of wounds, there are some key players which include inflammatory cytokines, e.g., IL-2, IL-6, and TNF- α . Group II showed an augmented concentration of IL-2 (18.75 ± 1.04 ng/mL) in comparison to group I, where the concentration was 5.24 ± 0.68 ng/mL. IL-2 levels declined in group III and group IV, i.e., they were

12.34 ± 0.43 ng/mL and 8.47 ± 0.56 ng/mL, respectively. These values were very close to those of group V (6.39 ± 0.79 ng/mL) (Figure 6A).

IL-6 levels were found to reduce after *S. bryopteris* treatment in group IV (7.57 ± 0.847 ng/mL), the value of which was quite close to that of IL-6 levels in group V (6.40 ± 0.79 ng/mL) and more significant than group III (13.44 ± 1.068 ng/mL). Meanwhile, group II showed decline in IL-6 concentration (22.07 ± 1.30 ng/mL), Figure 6B.

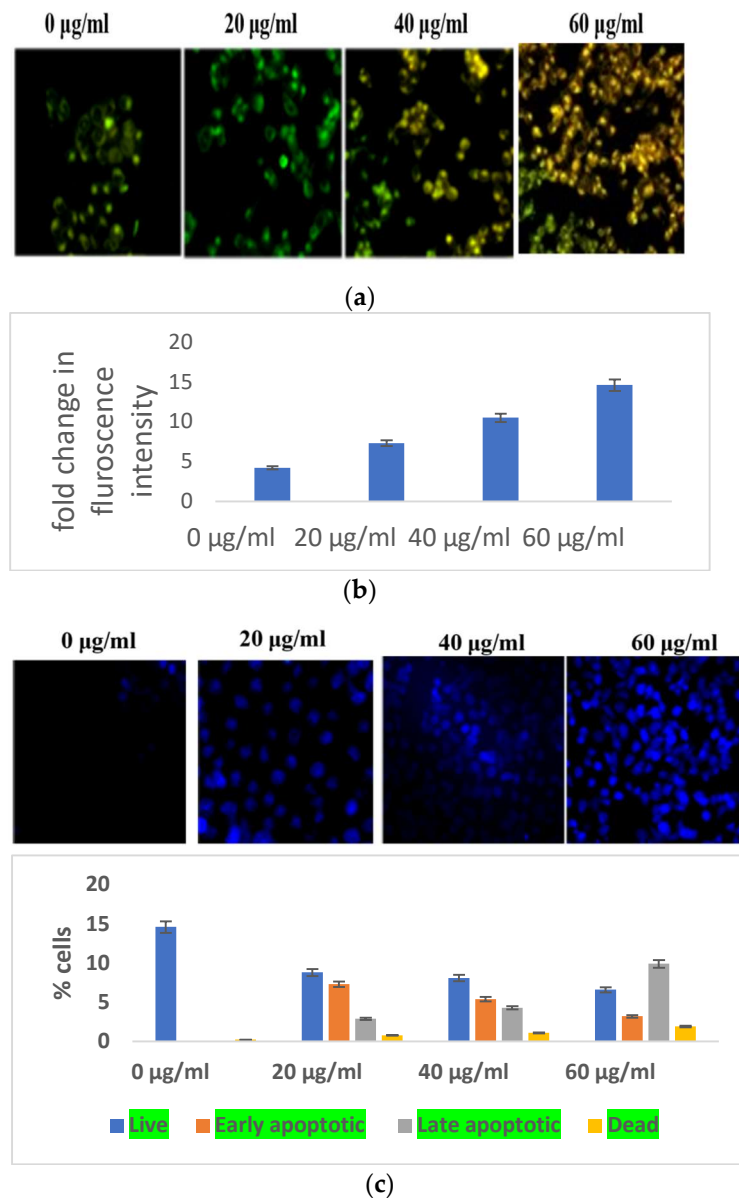


Figure 3. (a) Microscopic analysis of HaCaT cells in the presence/absence of *S. bryopteris* after dual staining of acridine orange and PI. (b) Nuclear condensation analysis of HaCaT cells in the presence/absence of *S. bryopteris*, as determined by DAPI staining. (c) Graphical representation of flow cytometric analysis.

All groups, except group I (509.54 pg/mL), had increased TNF-α levels. TNF-α levels decreased after *S. bryopteris* treatment in groups III (1735.57 pg/mL) and IV (934.098 pg/mL), although the results for these groups were similar to those of group V (723.546 pg/mL) in comparison to group II (2471.89 pg/mL), Figure 6C. In this study, there was a higher level of TNF-α expression in the STZ-induced negative control group as compared to the *S. bryopteris*-treated groups. The anti-inflammatory effects of interleukin-6 and interleukin-

2 on wound healing were diminished in the blood serum of the negative control group compared to the treatment groups.

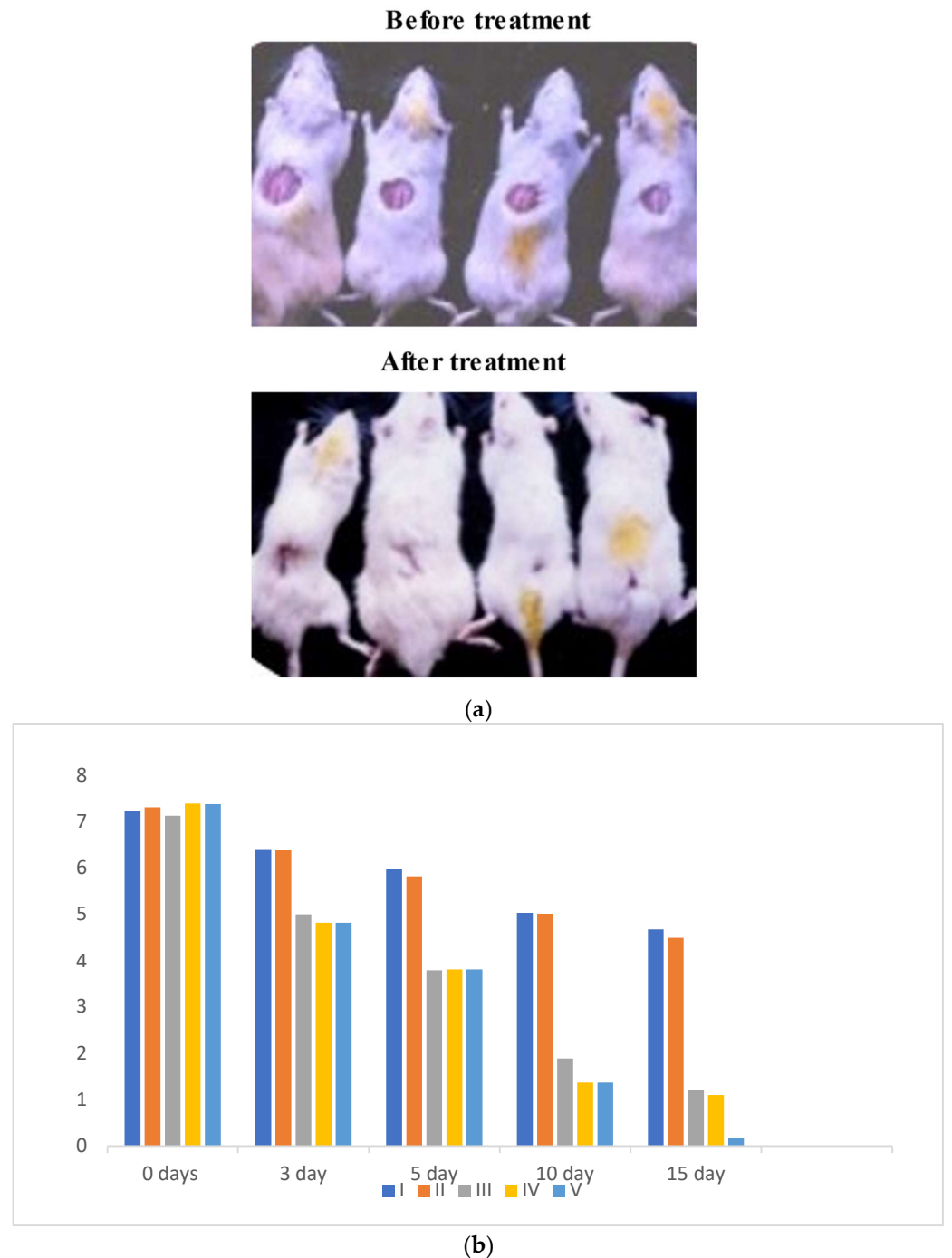
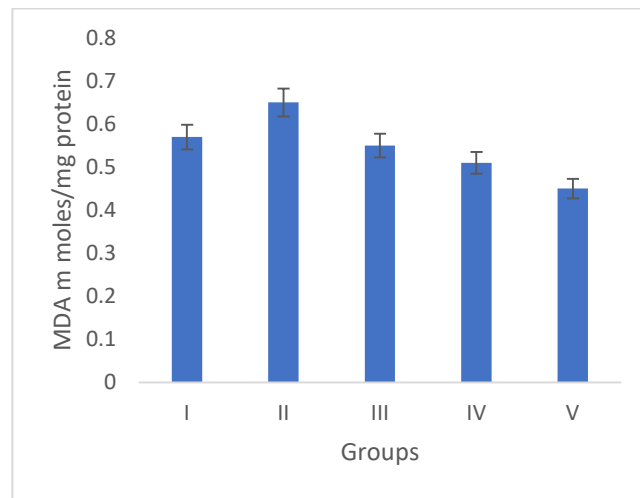
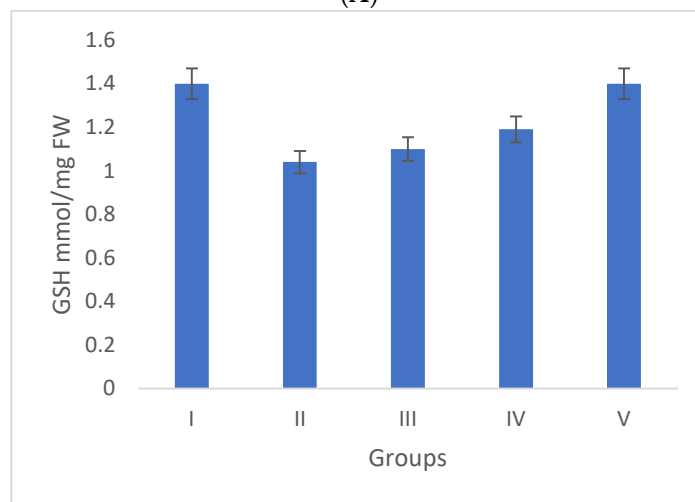


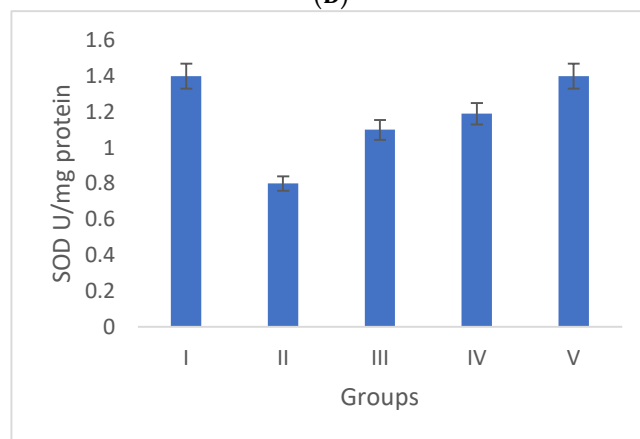
Figure 4. (a) Digital presentation of excision wounds in STZ-induced and normal control animals without treatment on day 0, 3, 5, 10, and 15 post-initiation of the wound. The progress of healing showed that healing was achieved by day 14 post-wound initiation and progressed to complete wound closure after 15 days in the flavonoid enriched fraction treated groups compared to the diabetic control, who remained unhealed after 15 days of treatment. (b) Graph of wound area analysis showing the decrease in wound size in diabetic-treated rats in a dose-dependent manner. The decrease was significant compared to the untreated diabetic control.



(A)

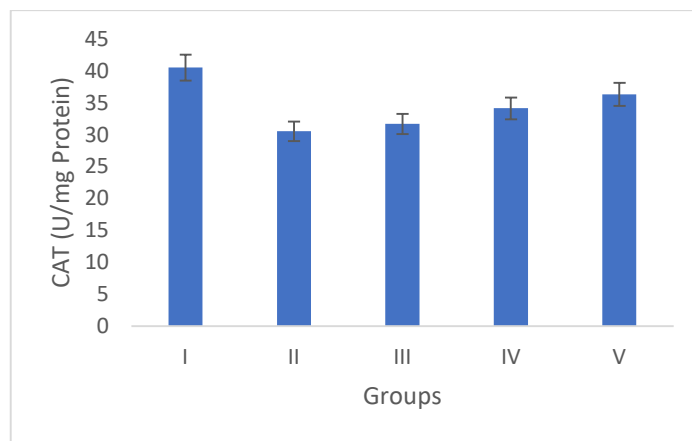


(B)



(C)

Figure 5. Cont.



(D)

Figure 5. Duncan’s multiple range test (DMRT) was used for the analysis. Bars with the same letters are not significantly different. All the values are means of five replicates ± SD. The parameter MDA, GSH, SOD, and CAT represent in images (A), (B), (C), and (D) respectively.

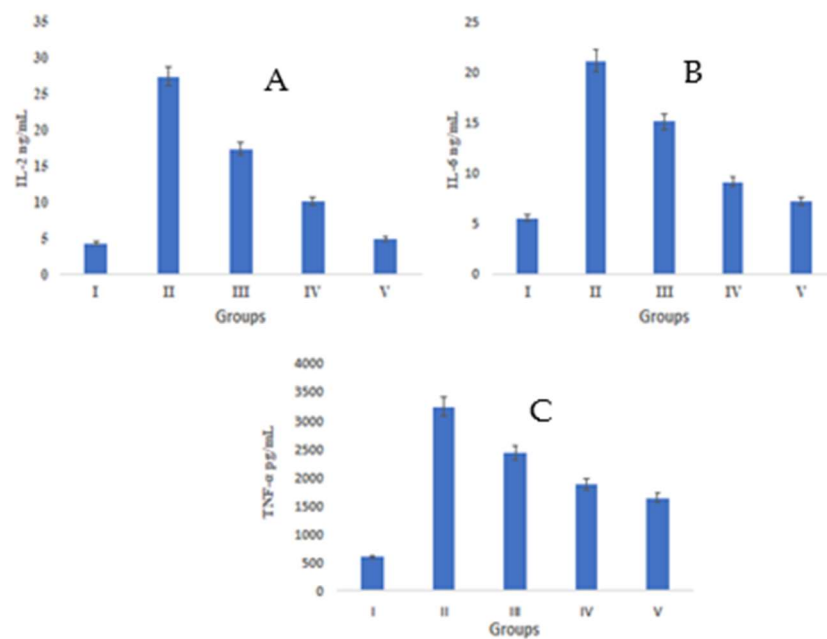
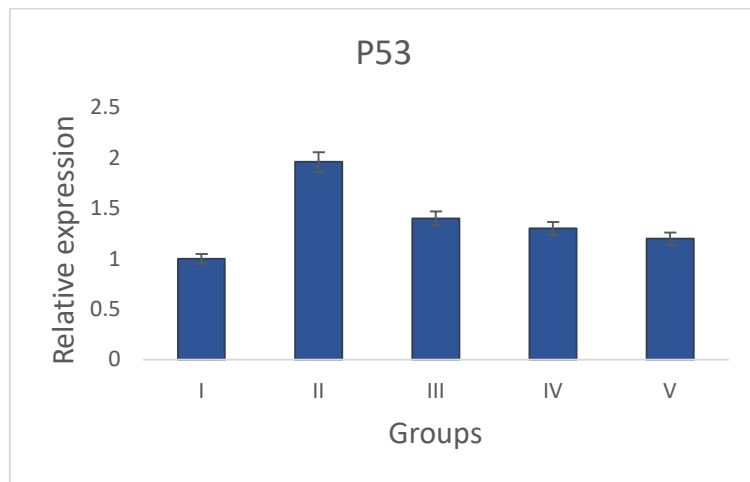


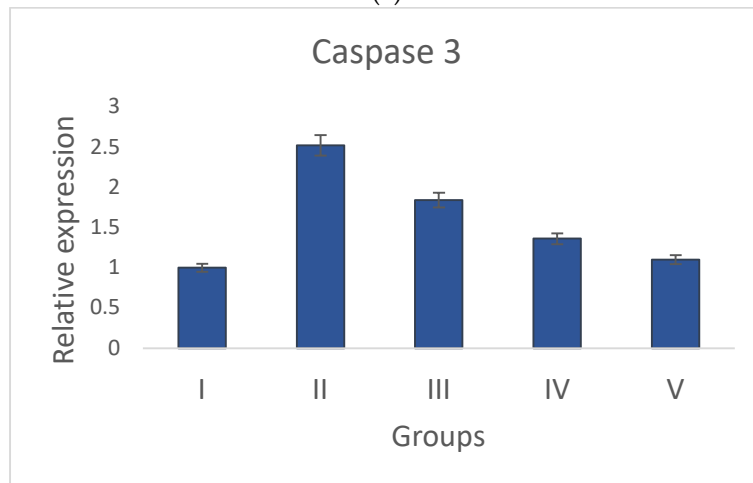
Figure 6. A Duncan’s multiple range test (DMRT) was applied for the study of the significant difference between the means ($p < 0.05$) for each parameter IL2, IL6, and TNF-alpha represent in images (A), (B), and (C) respectively. The difference between bars with the same letters is not significantly different. All data are means of five replicates ± SD.

3.3.3. Gene Expression Analysis of Bcl-2, p53, Bax, Caspase-3, and Caspase-9 by qRT-PCR

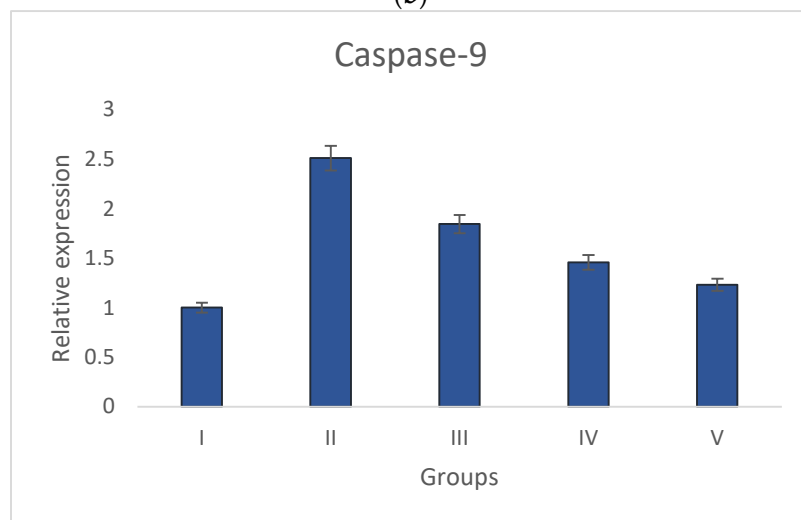
Groups I and II have increased levels of anti-apoptotic gene (Bcl-2) expression and decreased levels of pro-apoptotic gene expression (p53, caspase-3, Bax, and caspase-9). The pro-apoptotic and anti-apoptotic gene expression levels returned to normal in *S. bryopteris*-treated groups. These effects were comparable to those in group V who had received beta-dine treatment. Pro- and anti-apoptotic gene expression was examined using gene-specific primers. The GAPDH gene primer served as the endogenous control. The analyzed findings showed that, when compared to the STZ-induced group II animals, *S. bryopteris*-treated rats had higher expression levels of p53, Bax, caspase-3, caspase-9, Bcl-2, Figure 7a–e.



(a)



(b)



(c)

Figure 7. *Cont.*

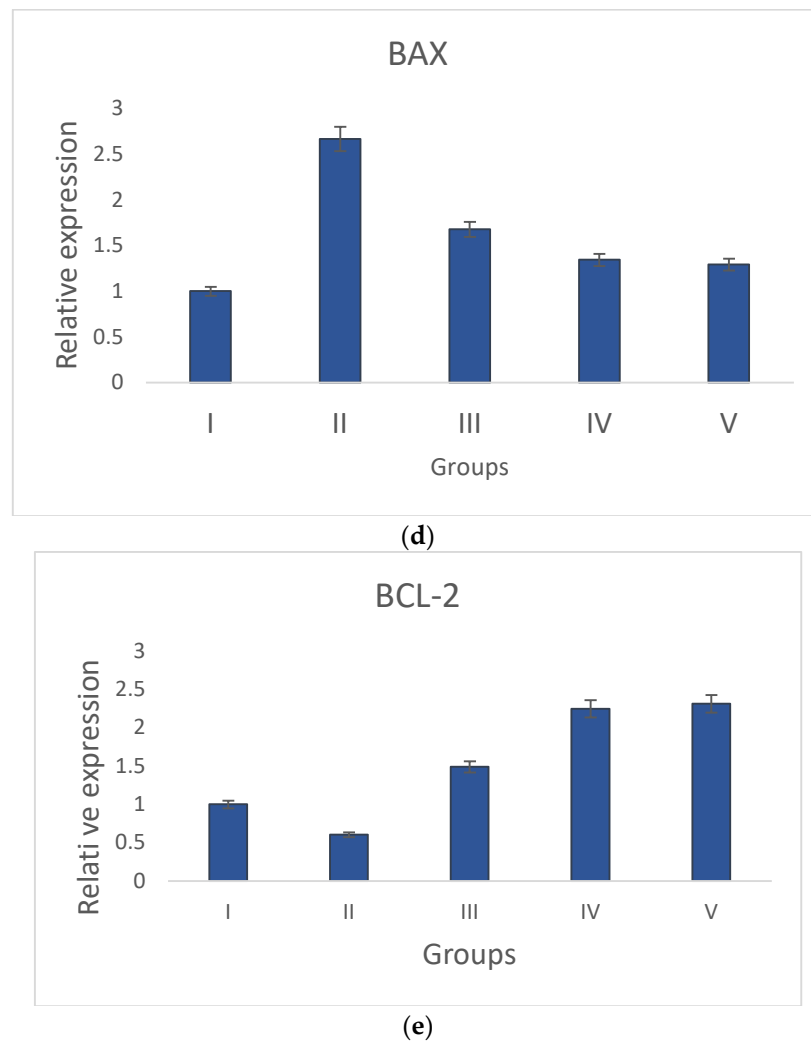


Figure 7. Relative expression of anti-apoptotic and pro-apoptotic genes determined by qRT-PCR in wounds induced by STZ. The relative expressions of pro-apoptotic genes (a) p53, (b) caspase-9, (c) Caspase-3, and (d) Bax were upregulated in all treatment groups when compared to the negative control group, while the relative expression of the anti-apoptotic gene (e) Bcl-2 was reduced in all treatment groups when compared to a higher upregulation in the negative control group.

After a preliminary analysis of the interleukin data using ELISA, molecular tests were conducted to assess the wound-healing capabilities of *S. bryopteris*. We looked at the expression of anti-apoptotic and pro-apoptotic genes to determine the mechanism by which *S. bryopteris* exerts its wound-healing effect. Cellular apoptosis can occur in two different ways: via intrinsic mitochondrial pathways or via an extrinsic death receptor mechanism. The process of mitochondria-mediated cell apoptosis is indicated by the up-regulation of p53 and the down-regulation of Bcl-2 mRNA. The progression of mitochondria-mediated apoptosis is demonstrated by the analysis of qRT-PCR, which demonstrated a higher expression of Bcl-2 and decreased expressions of p53, Bax, Caspase-3, and Caspase-9 in the negative control group and restored expressions in the treatment groups. In this route, Cyt-C produced from mitochondria interacts with BAX protein, which then binds to procaspase-9. Through the apoptosome, caspase-3, and caspase-9 participate in apoptosis Figure 7. *S. bryopteris* was identified in this investigation as an apoptotic activator.

3.4. Histopathological Analysis

A microscopic examination was performed with 40x magnification. Normal cells with a finely preserved granulated cytoplasm, as well as a clearly visible nucleus and nucleolus, were observed in Group I animals. Topical administration of *S. bryopteris* (0.5, 0.10%) to rat wound sites significantly reduced the wound diameter. Fast re-epithelialization of skin lesions was observed in Figure 8.

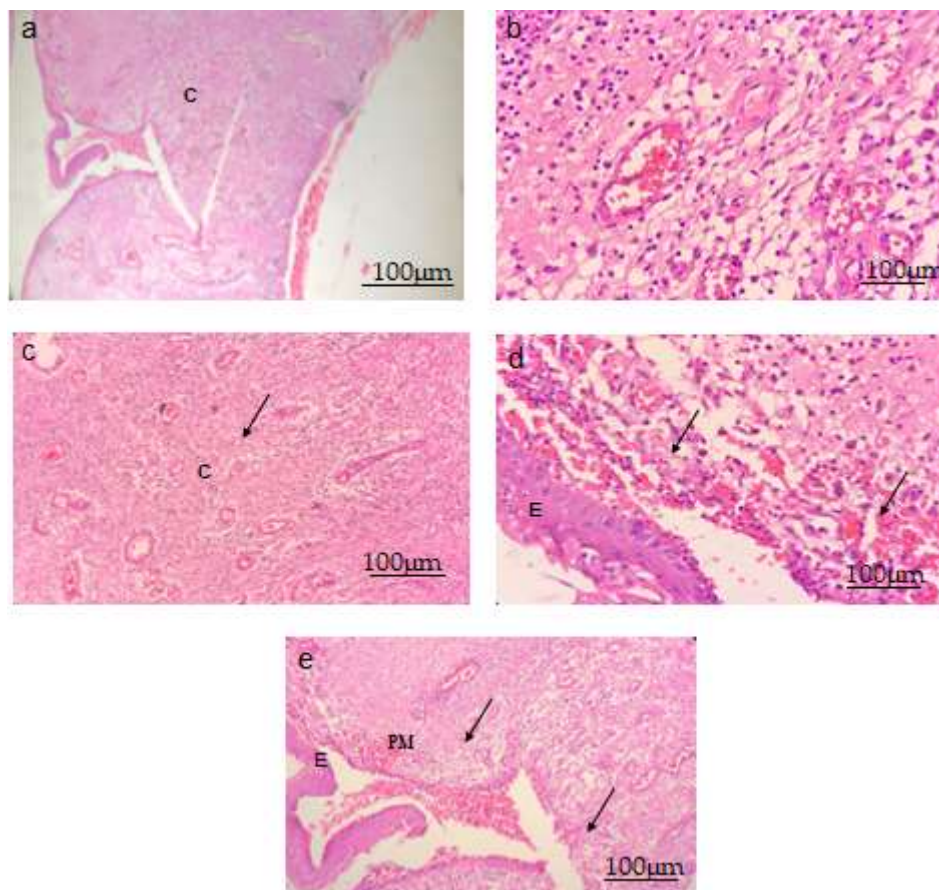


Figure 8. *S. bryopteris* improved the architecture of wounded tissue in (40×) H- and E-stained wounds. Scale bar 100 µm. (a) Normal control group, (b) negative control group, (c) a diabetic rat treated with 0.5% *S. bryopteris*, (d) a diabetic rat treated with 0.10% *S. bryopteris*, and (e) a diabetic rat treated with the standard (0.5% betadine). E: epidermis, C: collagen, PM: provisional matrix.

4. Concluding Remarks

A GCMS phytochemical analysis revealed imidazole, palmitic acid, amentoflavone, gallic acid, lupeol, L-fucitol, scyllo-inositol, and myoinositol as the significant phytoconstituents, which have previously been reported as wound healing phytomolecules present in another plant extracts in earlier research. Diabetes is induced by STZ, which is accelerated by an oxidative stress marker, and treatment normalizes and enhances enzymatic antioxidant defense systems such as GSH, SOD, CAT, and MDA. In diabetic wound healing, these defense systems protect keratinocytes from oxidative injury. The increased level of interleukin IL-2 and IL-6 tumor markers was observed in a dose-dependent manner, revealing their role in diabetic wound healing. The gene expression study of p53, Bcl-2, Bax, Caspase-3, and Caspase-9, and a qRT-PCR study of treated and untreated groups, indicated the progression of apoptotic pathways to block the course of wound healing. More research is being conducted to discover the distinct phytocompounds in treatment extracts that are responsible for wound healing. As a result, the current study indicated that the in vitro and in vivo efficacy of *S. bryopteris* requires clinical validation before it can be explored as a

potential wound-healing agent. It also causes apoptosis via the mitochondria-mediated death pathway.

Author Contributions: Conceptualization, A.G., V.K and C.V.R. and T.J.; methodology, V.K., L.A. and T.J.; software, M.M.K. and S.M.A.; validation, M.A. and A.A.; formal analysis, A.G., L.A. and O.A.A.-K.; investigation, A.G., V.K., M.M.K. and C.V.R.; resources, L.A., B.M. and S.M.A.; data curation, B.M., S.M.A. and M.K.; writing—original draft preparation, C.V.R., M.M.K., M.K., S.M. and A.A.; writing—review and editing, B.M., M.A., S.M.; visualization, M.K. and O.A.A.-K.; supervision, S.M., A.A. and O.A.A.-K.; project administration, M.A. and T.J.; funding acquisition, T.J. All authors have read and agreed to the published version of the manuscript.

Funding: This study is supported via funding from Prince Sattam bin Abdulaziz University project number (PSAU/2023/R/1444).

Institutional Review Board Statement: The study was approved by the Institutional Animal Ethics Committee(IAEC) National Botanical Research Institute (NBRI) Lucknow, India (BT/PR24882/NER/95/890/2017), dated 5 April 2019.

Data Availability Statement: The data presented in this study are available on request from the corresponding author.

Acknowledgments: The authors would like to thank the Director of CSIR, NBRI for providing the essential facilities for these experiments.

Conflicts of Interest: The authors declare no conflict of interest.

References

1. International Diabetes Federations. *IDF Diabetes Atlas*, 7th ed.; International Diabetes Federation: Brussels, Belgium, 2015.
2. Bhan, S.; Mitra, R.; Arya, A.K.; Pandey, H.P.; Tripathi, K. A study on evaluation of apoptosis and expression of bcl-2-related marker in wound healing of streptozotocin-induced diabetic rats. *Dermatology* **2013**, *2013*, 739054. [[CrossRef](#)] [[PubMed](#)]
3. Giannone, G.; Mazzone, O.; Russo, A.; Trovato, G.M. Electrocardiographic findings during colonoscopy. *Boll. Soc. Ital. Cardiol.* **1978**, *23*, 441–446. [[PubMed](#)]
4. Siqueira, M.F.; Li, J.; Chehab, L.; Desta, T.; Chino, T.; Krothpali, N.; Behl, Y.; Alikhani, M.; Yang, J.; Braasch, C.; et al. Impaired wound healing in mouse models of diabetes is mediated by TNF-alpha dysregulation and associated with enhanced activation of forkhead box O1 (FOXO1). *Diabetologia* **2010**, *53*, 378–388. [[CrossRef](#)] [[PubMed](#)]
5. Arya, A.K.; Pokharia, D.; Tripathi, K. Relationship between oxidative stress and apoptotic markers in lymphocytes of diabetic patients with chronic non healing wound. *Diabetes Res. Clin. Pract.* **2011**, *94*, 377–384. [[CrossRef](#)] [[PubMed](#)]
6. Chen, L. The worldwide epidemiology of type 2 diabetes mellitus—present and future 190 perspectives. *Nat. Rev. Endocrinol.* **2012**, *8*, 228–236. [[CrossRef](#)] [[PubMed](#)]
7. Li, A.; Wang, D.; Yu, B.; Yu, X.; Li, W. Maintenance or collapse: Responses of extraplastidic membrane lipid composition to desiccation in the resurrection plant *Paraisometrum mileense*. *PLoS ONE* **2014**, *9*, 103430. [[CrossRef](#)] [[PubMed](#)]
8. Sah, N.K.; Singh, S.N.P.; Sahdev, S.; Banerji, S.; Jha, V.; Khan, Z.; Hasnain, S.E. Indian herb ‘Sanjeevani’ (*Selaginella bryopteris*) can promote growth and protect against heat shock and apoptotic activities of ultra violet and oxidative stress. *J. Biosci.* **2005**, *30*, 499–505. [[CrossRef](#)] [[PubMed](#)]
9. Antony, R.; Thomas, R. A mini review on medicinal properties of the resurrecting plant *Selaginella bryopteris* (Sanjeevani). *Int. J. Pharm. Life Sci.* **2011**, *2*, 7.
10. Kunert, O.; Swamy, R.C.; Kaiser, M.; Presser, A.; Buzzi, S.; Rao, A.A.; Schühly, W. Anti-plasmodial and leishmanicidal activity of bioflavonoid from Indian *Selaginella bryopteris*. *Phytochem. Lett.* **2008**, *1*, 171–174. [[CrossRef](#)]
11. Paswan, S.K.; Gautam, A.; Verma, P.; Rao, C.V.; Sidhu, O.P.; Singh, A.P.; Srivastava, S. The Indian magical herb ‘Sanjeevani’ (*Selaginella bryopteris* L.)—a promising anti-inflammatory phytomedicine for the treatment of patients with inflammatory skin diseases. *J. Pharmacopunct.* **2017**, *20*, 93.
12. Sah, P. Does the magical himalayan herb “Sanjeevani Booti” really exist in nature. *J. Am. Sci.* **2008**, *4*, 65–67.
13. Ragazzi, E.; Veronese, G. Quantitative analysis of flavonoid compounds after thin layer chromatographic separation. *J. Chrom.* **1973**, *77*, 369–375. [[CrossRef](#)] [[PubMed](#)]
14. Oyaizu, M. Studies on products of browning reaction: Antioxidative activity of products of browning reaction. *J. Nutr. Diet* **1986**, *44*, 307–315. [[CrossRef](#)]
15. Bhatia, A.; Bharti, S.K.; Tripathi, T.; Mishra, A.; Sidhu, O.P.; Roy, R.; Nautiyal, C.S. Metabolic profiling of *Commiphora wightii* (guggul) reveals a potential source for pharmaceuticals and nutraceuticals. *Phytochemistry* **2015**, *110*, 29–36. [[CrossRef](#)]
16. Yadav, P.P.; Arora, A.; Bid, H.K.; Konwar, R.R.; Kanojiya, S. New cassane butenolide hemiketal diterpenes from the marine creeper *Caesalpinia bonduc* and their antiproliferative activity. *Tetrahedron Lett.* **2007**, *48*, 7194–7198. [[CrossRef](#)]

17. Besra, S.E.; Ray, M.; Dey, S.; Roy, S.; Deb, N. Apoptogenic activity of secretion extract of *Bellamyia Bengalensis f. annandalei* via mitochondrial mediated caspase cascade on human leukemic cell lines. *Int. J. Pharm. Sci. Rev. Res.* **2013**, *20*, 146–152.
18. Nikhil, K.; Sharan, S.; Chakraborty, A.; Bodipati, N.; Peddinti, R.K.; Roy, P. Role of isothiocyanate conjugate of pterostilbene on the inhibition of MCF-7 cell proliferation and tumor growth in Ehrlich ascitic cell induced tumor bearing mice. *Exp. Cell Res.* **2014**, *320*, 11–28. [[CrossRef](#)] [[PubMed](#)]
19. Kakkar, P.; Das, B.; Viswanathan, P.N. A modified spectrophotometric assay of superoxide dismutase. *Indian J. Biochem. Biophys.* **1984**, *21*, 130–132. [[PubMed](#)]
20. Aebi, H. Catalase. In *Methods of Enzymatic Analysis*; Academic Press: Weinheim, Duitsland; NewYork, NY, USA, 1974; pp. 673–684.
21. Ellman, G.L. Tissue sulfhydryl groups. *Arch. Biochem. Biophys* **1959**, *82*, 70–77. [[CrossRef](#)]

Disclaimer/Publisher’s Note: The statements, opinions and data contained in all publications are solely those of the individual author(s) and contributor(s) and not of MDPI and/or the editor(s). MDPI and/or the editor(s) disclaim responsibility for any injury to people or property resulting from any ideas, methods, instructions or products referred to in the content.